Bioorganic & Medicinal Chemistry Letters 19 (2009) 1512–1516

Contents lists available at ScienceDirect

Bioorganic & Medicinal Chemistry Letters

journal homepage: www.elsevier.com/locate/bmcl

Indolyl-pyrrolone as a new scaffold for Pim1 inhibitors

Stefania Olla [a], Fabrizio Manetti [a], Emmanuele Crespan [b], Giovanni Maga [b], Adriano Angelucci [c], Silvia Schenone [d], Mauro Bologna [c], Maurizio Botta [a,*]

[a] Dipartimento Farmaco Chimico Tecnologico, Università degli Studi di Siena, Via Alcide de Gasperi 2, I-53100 Siena, Italy
[b] Istituto di Genetica Molecolare, IGM-CNR, Via Abbiategrasso 207, I-27100 Pavia, Italy
[c] Dipartimento di Biologia di Base ed Applicata, Università degli Studi dell'Aquila, Via Vetoio, Loc. Coppito, I-67010 Coppito L'Aquila, Italy
[d] Dipartimento di Scienze Farmaceutiche, Università degli Studi di Genova, Viale Benedetto XV 3, I-16132 Genova, Italy

ARTICLE INFO

Article history:
Received 10 October 2008
Revised 22 December 2008
Accepted 6 January 2009
Available online 9 January 2009

Keywords:
Molecular docking
Pim1 kinase
Inhibitor
Pharmacophore modeling
Commercially available compounds

ABSTRACT

Pim1 belongs to a family of serine/threonine kinases, which is involved in the control of cell growth, differentiation, and apoptosis. Pim1 plays a pivotal role in cytokine signaling and is implicated in the development of a large number of tumors, representing a very attractive target for anticancer therapy. In this work, we applied a virtual screening protocol aimed at identifying small molecules able to inhibit Pim1 activity. The search of novel inhibitors was performed through a structure-based molecular modeling approach, taking advantage of the availability of the three-dimensional crystal structure of inhibitors bound to Pim1. Starting from the knowledge of protein–ligand complexes, the software LigandScout was used to generate pharmacophoric models, in turn used as queries to perform a virtual screening of databases, followed by docking experiments. As a result, a restricted set of candidates for biological testing was identified. Finally, among the six compounds selected as potential inhibitors of Pim1, two candidates endowed with a significant activity against Pim1 emerged. Interestingly, one of these compounds has a chemical scaffold different from inhibitors previously identified.

Pim1 is the first described member of a unique family of serine/threonine kinases which includes Pim2 and Pim3 with significant sequence homology to Pim1.[1–3] Pim1 is an oncogene[4] and was identified as a common integration site for Moloney Murine Leukemia Virus (MoMuLV), which may induce T cell lymphomas in mice.[5,6] Overexpression of Pim1 in mice resulted in susceptibility to lymphomagenesis, which is likely to occur through a synergistic effect between Pim1 and c-Myc.[7] In humans, the Pim-1 gene is expressed mainly in the developing fetal liver and spleen[8] and in hematopoietic malignancies.[9,10] Pim1 has been shown to have diverse biological roles in cell survival, proliferation, differentiation, and apoptosis.[11] Pim1 overexpression is observed in a range of human lymphomas,[12] several leukemias,[8] and also in prostate cancer.[13–15] Moreover, a number of somatic mutations and chromosomal translocations in Pim1[16] have been identified in lymphomas of the nervous system and AIDS-induced non-Hodgkins lymphoma[17] that probably affect Pim1 kinase activity or stability. In addition, overexpression of Pim1 in hemopoietic cells enhances cell survival, by protecting these cells from apoptosis induced by cytokine withdrawal,[18,19] glucocorticoids,[20] and genotoxic stress.[21] In light of their oncogenic potential, the Pim1 kinase is emerging as an important new target for drug discovery.[22]

To facilitate development of lead compounds, several groups have reported the crystal structure of Pim1 in complex with a number of ATP-mimetic kinase inhibitors with broad kinase inhibition profiles.[23–26] Interestingly, the crystal structures of Pim1 revealed an atypical sequence in the hinge region and an unique conformation that distinguish this protein from other structurally characterized kinases. In detail, one hydrogen bond between N1 of ATP and a protein backbone NH is highly conserved among protein kinases, while a proline (Pro123) residue occupies the same position of Pim1 sequence, with a consequent loss of any hydrogen bond with ATP. Considering that a proline residue at this position is rare, its presence suggests that the hydrogen bond to N1 of ATP is not necessary for substrate binding, and alternative interactions are sufficient to correctly position ATP within its binding site (as an example, van der Waals interactions with the hinge region serve to position the ligand).

To identify novel Pim1 inhibitors, we employed a structure-based virtual screening approach consisting in the application of different sequential filters based on pharmacophoric models, drug-like property calculations, and docking simulations. A pharmacophoric model was generated by means of a structure-based approach, codifying the interactions between ligands and the target protein. The pharmacophore was used as a three-dimensional query to screen a database of commercially available compounds to find putative hits to be purchased and submitted to biological

* Corresponding author. Tel.: +39 0577 234306; fax: +39 0577 234333.
E-mail address: botta@unisi.it (M. Botta).

0960-894X/$ - see front matter © 2009 Elsevier Ltd. All rights reserved.
doi:10.1016/j.bmcl.2009.01.005

assays. Six compounds were selected and tested, finding two of them able to inhibit Pim1 at a micromolar concentration.

The crystallographic structure of the complex between the human Pim1 and staurosporine (entry 1YHS of Protein Data Bank)[24] was chosen as a starting point to perform molecular modeling studies. The choice was based on the fact that, when we started with our work, staurosporine was the most potent inhibitor (0.01 μM) cocrystallized with the protein (Chart 1).[38] The structure of the complex was analyzed with LigandScout[27] to identify the chemical features important for ligand–enzyme interactions to be codified into a structure-based pharmacophoric model. In detail, information for the pharmacophore pattern (3D coordinates of interaction points) was obtained by interpretation of LigandScout pharmacophore definitions and resulted in specific interaction models that were able to map ligand in its bioactive conformation. LigandScout definition allows an atom or functional group to serve as root for multiple features thus resembling the situation in the binding pocket.

LigandScout classified the amino group at position 11 of staurosporine (Chart 1) as a hydrogen bond donor (toward Asp128 that could act as the hydrogen bond acceptor) or as a positively ionizable group (toward the carboxylate group of both Asp128 and Glu171 that could be the counterpart of a salt bridge). As a consequence, we decided to generate two different pharmacophoric models differing by a positively ionizable group (Fig. 1, upper) instead of a hydrogen bond donor (Fig. 1, bottom). The remaining features were three hydrophobic regions and a hydrogen bond donor, in addition to 13 excluded volume spheres that the software included automatically (Fig. 1).

The model shown in Figure 1 (bottom) is characterized by a hydrogen bond donor group corresponding to the lactam NH of staurosporine interacting with the backbone carbonyl group of Glu121. This interaction with the hinge region of Pim1 is described as a crucial key for activity of inhibitor. The second hydrogen bond donor is represented by the amino group at position 11 of staurosporine that contacts the terminal carboxy moiety of Asp128 (Fig. 1b). The same amino group can also act as a positively ionizable group interacting with both Asp128 and Glu171 (Fig. 1, upper). Two hydrophobic features of both pharmacophoric models were occupied by the external phenyl rings of staurosporine, while the remaining hydrophobic group corresponded to the methyl moiety of the methoxy group at position 10 of the ligand. Finally, the 13 excluded volumes reflect potential steric restrictions and correspond to the positions that are sterically claimed by macromolecular environment surrounding the ligand (namely, Leu44, Gly45, Phe49, Val52, Lys67, Arg122, Val126, Leu174, Ile175, Ile185, Asp186). Excluded volume spheres included in the model enhance steric selectivity, thus eliminating database compounds that are not allowed to penetrate these features.

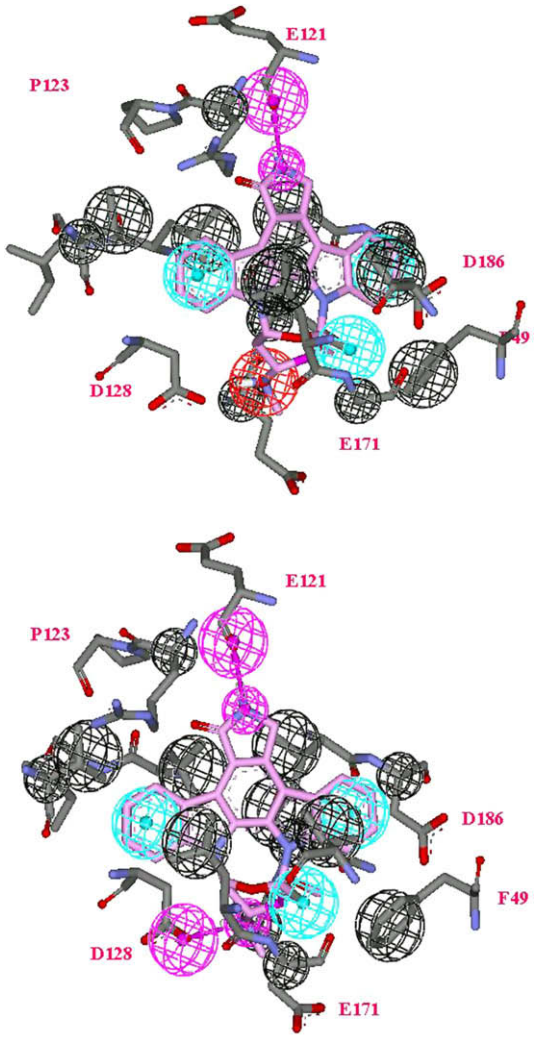

Figure 1. Graphical representation of the two structure-based pharmacophoric models generated by means of LigandScout. Pharmacophore with a positive ionizable group (upper) instead of a hydrogen bond acceptor feature (bottom).

To confirm the pharmacophoric features identified by LigandScout as important keys for interaction between Pim1 and its ligands, GRID[28] Molecular Interaction Fields (MIFs) were calculated for the region of the protein interacting with staurosporine. DRY (hydrophobic), N1 (neutral flat NH, e.g., amide), and N3+ (amine NH_3^+ cation) were selected as probes to explore hydro-

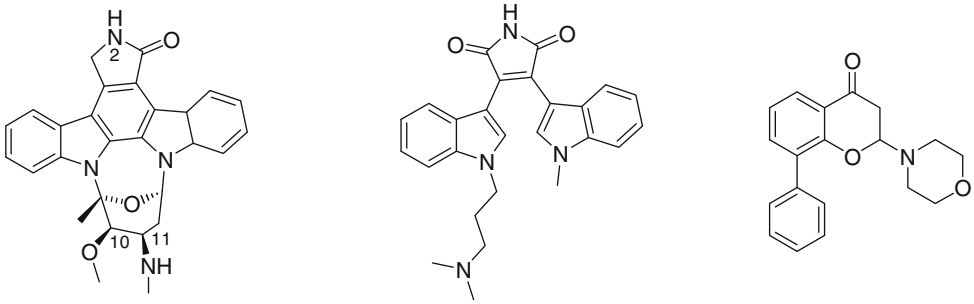

Chart 1. Structure of Pim1 inhibitors cocrystallized with the protein.

phobic interactions, to mimic hydrogen bond donor groups, and to find possible interactions with positive ionizable groups, respectively. Points of minimum of MIFs (i.e., the points in which the interaction energy assumes the lowest values) were calculated for each probe, thus identifying the regions of most favorable interactions with the protein (Fig. 2). As a result, the points of minimum of MIF corresponded to the pharmacophoric features identified by LigandScout.

Next, the two pharmacophoric models were imported in Catalyst[29] and used to perform an in silico database screening.

The two structure-based pharmacophoric models were combined with docking techniques for the virtual screening of the Asinex Gold Collection, a database consisting of over 200,000 commercially available compounds.[30] Structure-based virtual screening usually involves only the docking of compounds into a protein binding site by using docking algorithms, followed by scoring and ranking of compounds to identify potential hits. However, several recent studies have shown that pharmacophore-based filtration in addition to docking-based virtual screening can significantly improve the probability of identifying suitable candidates.[31,32] The steps of the in silico screening protocol are summarized as follows. The pharmacophoric hypotheses were applied as the first filter to screen the whole Asinex database, retaining all the compounds able to map at least three out of the five features, but only one of the hydrophobics. Next, the number of rotatable bonds (cutoff set to 10) and the Fast Fit value (cutoff set to 1.5) were used as sequential filters to remove too flexible and/or poorly fitting entries, respectively. An additional filter based on the Lipinski's rule of five[33] was applied. Finally, the resulting compounds were submitted to docking simulations.

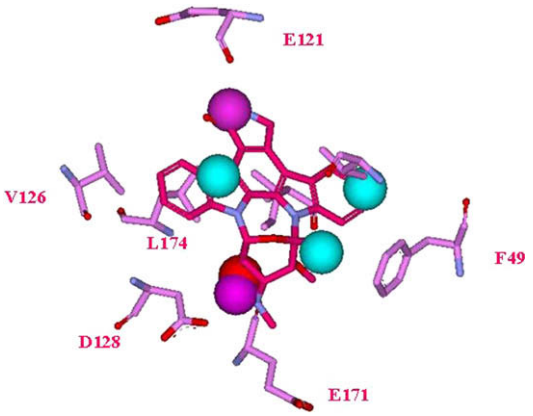

Figure 2. Graphical representation of the most favorable interaction points between the selected probes (DRY in cyan, N1 in magenta, and N3+ in red) and the residues of Pim1. These points confirmed the features identified by LigandScout.

Crystal structures of Pim1 in complex with known inhibitors (Chart 1) were used to establish the most suitable settings for docking experiments and to assess the reliability of the docking protocol (see Supplementary Material). Docking calculations were carried out in two consecutive steps, in such a way to optimize the balance between the quality of docking and the time required for calculations. Accordingly, two different programs were employed. In the first step, compounds deriving from database filtration were analyzed with GOLD,[34] retaining only compounds with a score of 30 or higher (the choice of this cutoff value was driven by the score between 31 and 47 found for known inhibitors) and appropriate binding (in terms of interactions with the protein). Resulting compounds were then submitted to Autodock[35] calculations leading to the final list of six entries to be purchased and tested (different parameters were taken into account for the final selection, such as docking score, energy of binding, structural diversity, and commercially availability of the appropriate amount for biological tests).

Selected compounds (Chart 2) were submitted to a preliminary biological assay to evaluate the percent inhibition of Pim1 activity at 100 μM.[36] IC_{50} values were determined only for compounds able

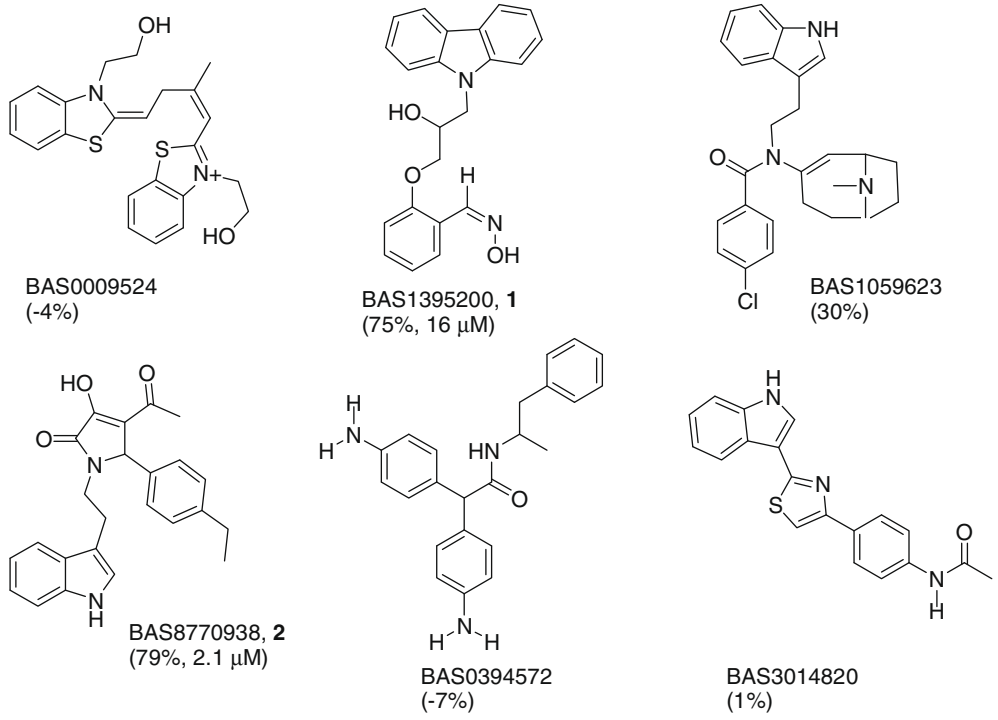

Chart 2. Structure of compounds selected by means of the virtual screening protocol. Percent inhibition of Pim1 activity (single dose, 100 μM) and IC_{50} values are reported in parentheses.

to reduce significantly Pim1 activity. As a result, BAS1395200 (**1**) and BAS8770938 (**2**) with a 75% and 79% inhibition, respectively, showed IC_{50} of 16 and 2.1 μM, respectively.

Compound **2** was also evaluated for its antiproliferative effect on prostate cancer cell lines PC3 and LNCaP. These cells express Pim1 and demonstrated to be sensitive to the treatment of specific Pim1 inhibitors.[37] Cells were treated with increasing concentrations of **2** and were counted after 72 h. Both cell lines appeared to be influenced by **2** in their proliferative potential (Fig. 3a). In fact, **2** determined a significant reduction in cell number with a similar IC_{50}: 10.1 ± 0.6 μM in PC3 cells and 10.6 ± 0.2 μM in LNCaP cells. The cytofluorimetric analysis revealed that the inhibition in cell proliferation was associated to a block of cells in S and G2/M phases (Fig. 3b).

On the basis of biological results, **1** and **2** were used as the substructures to search their analogues within the Asinex database, resulting in six additional compounds (structures and biological data are reported in Table 1). Several of them maintained affinity at micromolar concentrations, ranging from 2.1 (**2**) to 4.5 μM (**8**). Compounds **2**–**8** were also tested for their ability to inhibit Pim-1 kinase activity in vitro, following a protocol reported in Supplementary Material. As a result, they showed ID_{50} values comprised from 4.5 (**2**) to 19 μM (**7**).

Moreover, kinase activity assays in the presence of different amount of inhibitors and increasing ATP concentrations were performed to determine the inhibition mechanism. Data analysis showed that all of these compounds were competitive inhibitors toward ATP (data not shown).

Pyrrolone derivatives similar to **2** were previously reported as hits for different targets. As examples, they were found to be antagonists of CCR4,[39] vasopressin-2 receptor,[40] and formylpeptide receptor[41] as well as inhibitors for ubiquitin C-terminal hydrolase-L3,[42] HIV-1 integrase,[43] and bacterial glucosamine-6P synthase.[44]

Although such compounds contain a potentially unstable and reactive Michael-acceptor ring at their core, none of these previous reports investigated on their chemical and biological stability. However, a pyrrolone analogue was identified as a CCR4 antagonist within a 'clean' database previously pruned for potentially reactive and undesirable molecules.[39]

Table 1
Structure and inhibitory activity of compounds **2**–**8** toward Pim1 kinase

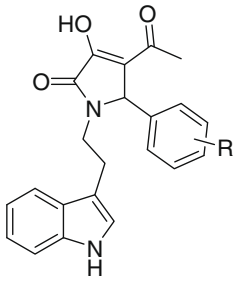

Compound[a]	R	Percent inhibition[b]	K_i (μM)[b]	ID_{50} (μM)[c]
2, BAS8770938	4-Et	79	2.1 ± 0.3	4.5 ± 0.7
3, BAS8770931	4-Me	54	ND	10 ± 2
4, BAS8770945	4-COOMe	57	ND	13 ± 2
5, BAS8770951	4-OEt	71	4.2 ± 0.5	12 ± 4
6, BAS8770954	4-OH	92	2.2 ± 0.4	5.2 ± 1.1
7, BAS8770957	3-OH	84	ND	19 ± 4
8, BAS8770949	3-OMe, 4-OH	90	4.5 ± 0.7	9.5 ± 1.7

[a] Compounds purchased from Asinex.
[b] Percent inhibition was determined at 100 μM. Enzyme assay was carried out by Cerep[36] on human recombinant Pim1 kinase using staurosporine as reference compound (further detail on Supplementary data).
[c] In vitro inhibition of Piml kinase activity. Further details on Supplementary Material.

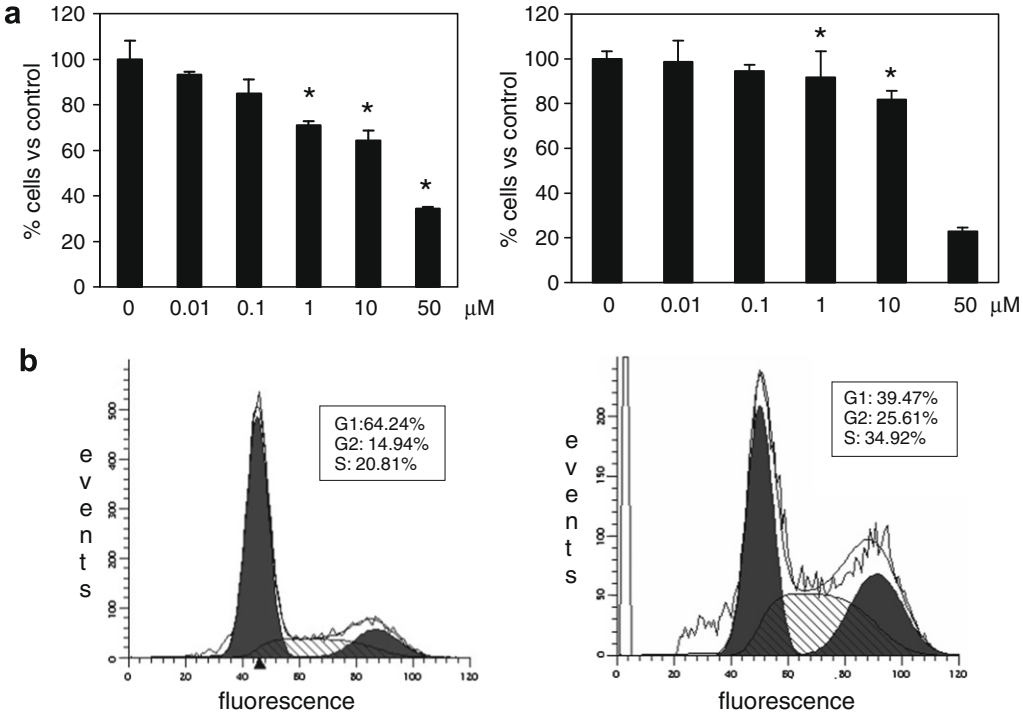

Figure 3. (a) Compound **2** inhibits the growth of prostate cancer cells PC3 and LNCaP. Growth inhibition by **2** was evaluated after 72 h and was reported as percentage of live cells with respect to the control (100%). Each measure is the mean of triplicate determinations (± SD). *P* values were calculated by *t* tests. $^{*}P < 0.01$. (b) PC3 cells treated for 72 h with 10 μM **2** were analyzed by cytofluorimetry and percentage of cells in each phase of the cell cycle was determined.

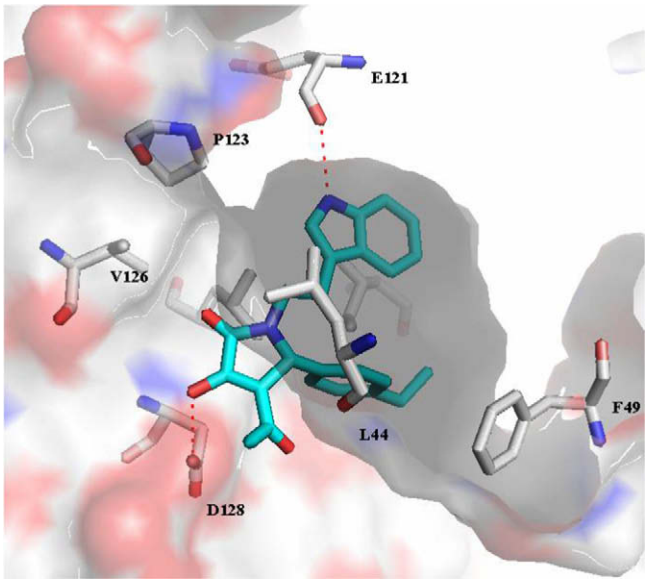

Figure 4. Graphical representation of the binding mode of **2** within the Pim1 binding site.

Purity of pyrazolone derivatives was reported by Asinex ranging from 93% to 99%. To check for this degree of purity, we perform a HPLC analysis of compounds after shipping and storage. Solutions were analyzed, finding percent purity values comparable to those reported by Asinex and ranging from 92% to 98%. The same analysis was not performed to check for compound stability upon exposure to the assay conditions. ^{1}H NMR spectra were recorded to confirm that compounds have the reported structure.

Analysis of docked complexes between Pim1 and the new inhibitors (**2** and its analogues) suggested that the inhibitors may exhibit a common orientation within the binding site. The predicted binding mode of the minimum energy conformation of **2** (Fig. 4) showed its indolic NH group in a hydrogen bond contact with Glu121 (a crucial interaction for the binding with the protein, also found in all the known inhibitors cocrystallized with Pim1). A second hydrogen bond interaction was present between the hydroxy group of **2** and Asp128. Moreover, hydrophobic interactions between Val52, Ala65, Ile104, Ile185 and the indole ring, as well as between Leu44, Phe49, Val52 and the phenyl group of the ligand, were found.

In conclusion, we report the application of a fast computational protocol based on structure-based pharmacophores for Pim1 inhibitors that was used to screen a large chemical database, leading to select entries with a significant inhibitory activity. In particular, **2** and its analogues showed chemical structures unrelated to any known class of Pim1 inhibitors and exhibited inhibitory activity in the micromolar range. Following these promising results, further studies are in progress to develop second generation compounds with improved activity.

Acknowledgment

Asinex is gratefully acknowledged for a partial financial support.

Supplementary data

Supplementary data associated with this article can be found, in the online version, at doi:10.1016/j.bmcl.2009.01.005.

References and notes

1. van der Lugt, N. M.; Domen, J.; Verhoeven, E.; Linders, K.; van der Gulden, H.; Allen, J.; Berns, A. *EMBO J.* **1995**, *14*, 2536.
2. Feldman, J. D.; Vician, L.; Crispino, M.; Tocco, G.; Marcheselli, V. L.; Bazan, N. G.; Baudry, M.; Herschman, H. R. *J. Biol. Chem.* **1998**, *273*, 16535.
3. Mikkers, H.; Allen, J.; Knipscheer, P.; Romeyn, L.; Hart, A.; Vink, E.; Berns, A. *Nat. Genet.* **2002**, *32*, 153.
4. Saris, C. J.; Domen, J.; Berns, A. *EMBO J.* **1991**, *10*, 655.
5. Cuypers, H. T.; Selten, G.; Quint, W.; Zijlstra, M.; Maandag, E. R.; Boelens, W.; van Wezenbeek, P.; Melief, C.; Berns, A. *Cell* **1984**, *37*, 141.
6. van Lohuizen, M.; Verbeek, S.; Krimpenfort, P.; Domen, J.; Saris, C.; Radaszkiewicz, T. G.; Berns, A. *Cell* **1989**, *56*, 673.
7. Selten, G.; Cuypers, H. T.; Berns, A. *EMBO J.* **1985**, *4*, 1793.
8. Amson, R.; Sigaux, F.; Przedborski, S.; Flandrin, G.; Givol, D.; Telerman, A. *Proc. Natl. Acad. Sci. U.S.A.* **1989**, *86*, 8857.
9. Meeker, T. C.; Nagarajan, L.; ar-Rushdi, A.; Rovera, G.; Huebner, K.; Croce, C. M. *Oncogene Res.* **1987**, *1*, 87.
10. Nagarajan, L.; Louse, E.; Tsujimoto, Y.; ar-Rushdi, A.; Huebner, K.; Croce, C. M. *Proc. Natl. Acad. Sci. U.S.A.* **1986**, *83*, 2556.
11. Wang, Z.; Bhattacharya, N.; Weaver, M.; Petersen, K.; Meyer, M.; Gapter, L.; Magnuson, N. S. *J. Vet. Sci.* **2001**, *2*, 167.
12. Yoshida, S.; Kaneita, Y.; Seto, M.; Mori, S.; Moriyama, M. *Oncogene* **1999**, *8*, 7994.
13. Dhanasekaran, S. M.; Barrette, T.; Ghosh, D.; Shah, R.; Varambally, S.; Kurachi, K.; Pienta, K. J.; Rubin, M. A.; Chinnaiyan, M. A. *Nature* **2001**, *412*, 822.
14. Ellwood-Yen, K.; Graeber, T. G.; Wongvipat, J.; Iruela-Arispe, M. L.; Zhang, J.; Matusik, R.; Thomas, G. V.; Sawyers, C. L. *Cancer Cell* **2003**, *4*, 223.
15. Chen, W. W.; Chan, D. C.; Donald, C.; Lilly, M. B.; Kraft, A. S. *Mol. Cancer Res.* **2005**, *3*, 443.
16. Pasqualucci, L.; Neumeister, P.; Goossens, T.; Nanjangud, G.; Chaganti, R. S.; Kupers, R.; Dalla-Favera, R. *Nature* **2001**, *412*, 341.
17. Akasaka, H.; Akasaka, T.; Kurata, M.; Ueda, C.; Shimizu, A.; Uchiyama, T.; Ohno, H. *Cancer Res.* **2000**, *60*, 2335.
18. Lilly, M.; Sandholm, J.; Cooper, J. J.; Koskinen, P. J.; Kraft, A. *Oncogene* **1999**, *18*, 4022.
19. Shirogane, T.; Fukada, T.; Muller, J. M.; Shima, D. T.; Hibi, M.; Hirono, T. *Immunity* **1999**, *11*, 709.
20. Moray, T.; Grzeschiczek, A.; Petzold, S.; Hartmann, H. U. *Proc. Natl. Acad. Sci. U.S.A.* **1993**, *90*, 10734.
21. Pircher, T. J.; Zhao, S.; Geiger, J. N.; Joneja, B.; Wojchowski, D. M. *Oncogene* **2000**, *19*, 3684.
22. Bullock, A. N.; Debreczeni, J. E.; Fedorov, O. Y.; Nelson, A.; Marsden, B. D.; Knapp, S. *J. Med. Chem.* **2005**, *48*, 7604.
23. Kumar, A.; Mandiyan, V.; Suzuki, Y.; Zhang, C.; Rice, J.; Tsai, J.; Artis, D. R.; Ibrahim, P.; Bremer, R. *J. Mol. Biol.* **2005**, *348*, 183.
24. Jacobs, M. D.; Black, J.; Futer, O.; Swenson, L.; Hare, B.; Fleming, M.; Saxena, K. *J. Biol. Chem.* **2005**, *280*, 13728.
25. Qian, K. C.; Wang, L.; Hichey, E. R.; Studts, J.; Barringer, K.; Peng, C.; Kronkaitis, A.; Li, J.; White, A.; Mische, S.; Farmer, B. *J. Biol. Chem.* **2005**, *280*, 6130.
26. Bullock, A. N.; Debreczeni, J.; Amos, A. L.; Knapp, S.; Turk, B. E. *J. Biol. Chem.* **2005**, *280*, 41675.
27. Wolber, G.; Langer, T. *J. Chem. Inf. Model.* **2005**, *45*, 160.
28. GRID 22; Molecular Discovery Ltd, 215 Marsh Road, Pinner, Middlesex, UK.
29. Catalyst, version 4.10; Accelrys Inc.: San Diego, CA, 2006.
30. Further information at the Web site http://www.asinex.com/prod/gold.html.
31. Polgar, T.; Keseru, G. M. *J. Med. Chem.* **2005**, *48*, 3749.
32. Evers, A.; Klabunde, T. *J. Med. Chem.* **2005**, *48*, 1088.
33. Lipinski, C. A.; Lombardo, F.; Dominy, B. W.; Feeney, P. *Adv. Drug Delivery Rev.* **1997**, *23*, 3.
34. Jones, G.; Willet, P.; Glen, R. C.; Leach, A. R.; Taylor, R. *J. Mol. Biol.* **1997**, *267*, 727.
35. Morris, G. M.; Goodsell, D. S.; Halliday, R. S.; Huey, R.; Hart, W. E.; Belew, R. K.; Olson, A. J. *J. Comput. Chem.* **1998**, *19*, 1639.
36. Further information at the Web site http://www.cerep.fr.
37. Holder, S.; Zemskova, M.; Zhang, C.; Tabrizizad, M.; Bremer, R.; Neidigh, J. W.; Lilly, M. B. *Mol. Cancer Ther.* **2007**, *6*, 163.
38. Before the completion of the present work, Tong Y. and coworkers (Tong, Y.; Stewart, K. D.; Thomas, S.; Przytulinska, M.; Johnson, E. F.; Klinghofer, V.; Leverson, J.; McCall, O.; Soni, N. B.; Luo, Y.; Lin, N. H.; Sowin, T. J.; Giranda, V. L.; Penning, T. D. *Bioorg. Med. Chem. Lett.* **2008**, *18*, 5206) reported a new series of isoxazolo-quinolines as additional Pim1 inhibitors.
39. Bayry, J.; Tchilian, E. Z.; Davies, M. N.; Forbes, E. K.; Draper, S. J.; Kaveri, S. V.; Hill, A. V. S.; Kazatchkine, M. D.; Beverley, P. C. L.; Flower, D. R.; Tough, D. F. *Proc. Natl. Acad. Sci. U.S.A.* **2008**, *105*, 10221.
40. Yangthara, B.; Mills, A.; Chatsudthipong, V.; Tradtrantip, L.; Verkman, A. S. *Mol. Pharmacol.* **2007**, *72*, 86.
41. Edwards, B. S.; Bologa, C.; Young, S. M.; Balakin, K. V.; Prossnitz, E. R.; Savchuck, N. P.; Sklar, L. A.; Oprea, T. I. *Mol. Pharmacol.* **2005**, *68*, 1301.
42. Hirayama, K.; Aoki, s.; Nishikawa, K.; Matsumoto, T.; Wada, K. *Bioorg. Med. Chem.* **2007**, *15*, 6810.
43. Dayam, R.; Al-Mawsawi, L. Q.; Neamati, N. *Bioorg. Med. Chem. Lett.* **2007**, *17*, 6155.
44. Floquet, N.; Richez, C.; Durand, P.; Maigret, B.; Badet, B.; Badet-Denisot, M.-A. *Bioorg. Med. Chem. Lett.* **2007**, *17*, 1966.